Res Chem Intermed (2015) 41:5007–5032
DOI 10.1007/s11164-014-1584-y

ORIGINAL PAPER

Electrochemical and surface analytical studies of carbon steel protected from corrosion in a low-chloride environment containing a phosphonate-based inhibitor

D. Sarada Kalyani · S. Srinivasa Rao · M. Sarath Babu · B. V. Appa Rao · B. Sreedhar

Received: 21 August 2013 / Accepted: 5 March 2014 / Published online: 25 March 2014

Abstract Electrochemical and surface analytical techniques have been used to study carbon steel protected from corrosion by use of a new ternary inhibitor formulation containing nitrilotris(methylenephosphonic acid) (NTMP), zinc ions, and nicotinic acid (NA). Potentiodynamic polarization studies indicate that the ternary inhibitor acts as a mixed-type inhibitor. Electrochemical impedance studies imply formation of a protective film at the metal–solution interface. Surface analysis by X-ray photoelectron spectroscopy (XPS) showed that the protective surface film contains Fe, Zn, P, N, C, and O. On the basis of shifts in the binding energies of these elements, it is inferred that the protective film comprises a multiligand complex, Fe(III), Zn(II)–NTMP–NA, $Zn(OH)_2$, and smaller quantities of oxides and/or hydroxides of iron. Analysis of the protective film by Fourier-transform infrared spectroscopy also supports this interpretation of the XPS results. Surface morphology and topography were studied by scanning electron microscopy and atomic force microscopy, respectively. On the basis of the results from all these

D. Sarada Kalyani · S. Srinivasa Rao (✉)
Department of Chemistry, V. R. Siddhartha Engineering College (Autonomous), Vijayawada 520007, Andhra Pradesh, India
e-mail: chemysri@yahoo.com; ssrnitw@gmail.com

M. Sarath Babu
Department of Chemistry, MIC College of Technology, Kanchikacherla, Vijayawada, Andhra Pradesh, India

B. V. Appa Rao
Department of Chemistry, National Institute of Technology, Warangal 506004, Andhra Pradesh, India

B. Sreedhar
Inorganic and Physical Chemistry Division, Indian Institute of Chemical Technology, Hyderabad, Andhra Pradesh, India

studies, a plausible mechanism for inhibition of corrosion by the formulation is proposed.

Keywords Protective film · Electrochemical studies · Carbon steel · Nicotinic acid · Surface analysis · NTMP

Introduction

Carbon steel is an important construction material with many industrial applications, especially cooling-water systems, because of its ease of fabrication and low cost. Corrosion of carbon steel is a major challenge in such systems, however. Phosphonate-based formulations are highly effective in control of corrosion of carbon steel in cooling-water systems [1–12]. In these formulations, a phosphonic acid and zinc ions act synergistically against corrosion. However, they require high concentrations of both components and the presence of toxic metal ions, for example Zn^{2+}, at high concentrations in industrial wastewaters is objectionable, according to environmental regulations. Although the effect of phosphonic acids on the environment has been reported to be negligible at the concentrations used for corrosion inhibition [13, 14], it is essential to reduce the concentration of zinc ions in phosphonic acid–Zn^{2+} formulations if they are to be applied in closed circuits, for example cooling-water systems. An effective means of overcoming this challenge is to add another non-toxic organic or inorganic compound to the phosphonic acid–Zn^{2+} binary formulations which acts synergistically in controlling corrosion at relatively low concentrations of both phosphonic acid and zinc ions. A few such formulations, known as ternary inhibitor formulations, have been reported in the literature [15–19]. Among several phosphonic acids, nitrilotris(methylenephosphonic acid) (NTMP) has been extensively studied for its corrosion-inhibition properties and has gained commercial importance over the past two decades. A brief review of literature reports of studies of NTMP as corrosion inhibitor is presented below.

NTMP-based corrosion inhibitor formulations

NTMP has three phosphonic acid groups and a nitrogen atom containing lone pair of electrons. In combination with specific metal ions it is reported to have excellent corrosion-inhibitive properties. Demadis et al. studied the organic–inorganic hybrids formed by NTMP with Zn^{2+} and concluded that they react with each other in 1:1 ratio by replacing the two of the six phosphonic acid protons; the amino nitrogen retains its proton, forming a zwitterion. The structure is concluded to be a polymeric material which is mainly responsible for the anticorrosion properties of NTMP [20]. Gonzalez et al. used electrochemical and surface analytical techniques to study the synergistic effect between zinc chloride and NTMP [21]. They inferred formation of a chelate compound by NTMP and zinc ions, which is responsible for enhancement of corrosion protection. Nakayama studied the inhibitory effects of NTMP on cathodic reactions of steels in saturated solutions of calcium hydroxide [22].

Formation of a polymer cross-linked by a calcium ion through three phosphono groups of NTMP was inferred from X-ray photoelectron spectroscopic (XPS) and Fourier transform infrared (FTIR) spectroscopic studies. Fang et al. [23] studied the passive films formed by five phosphonic acids and concluded that NTMP is more effective than four other phosphonic acids considered in their study. According to these researchers, an anticorrosive complex film is formed on the mild steel surface in the presence of NTMP. Labjar et al. [24] studied the corrosion inhibition of carbon steel and the antibacterial properties of NTMP. They inferred that NTMP is a mixed type inhibitor which is adsorbed on the surface, mainly by physisorption. NTMP and nitrilotriacetic acid (NTA) were evaluated as corrosion inhibitors for mild steel in sea water by Kar and Gurmeet Singh [25]. The authors concluded that NTMP performs better than NTA in corrosion inhibition because of formation of stable complexes by NTMP on the metal surface. The effect of phosphonates on corrosion of carbon steel in heat-supply water has also been reported [26]. It was inferred that formation of a zinc–phosphonate complex on the surface was responsible for control of anodic reactions. Wang et al. investigated the protective nature of NTMP layers adsorbed on AA6061 aluminium alloy [27]. They analysed the aluminium surface by use of XPS and FTIR.

With this background, the authors of this study report an environmentally friendly organic compound, nicotonic acid, as a new synergist to the binary inhibitor system containing NTMP and zinc ions [28]. In the presence of nicotinic acid (NA), the minimum concentrations of both NTMP and zinc ions required for effective corrosion inhibition could be substantially reduced, as was determined by gravimetric studies. The effects of pH, longer immersion period, and hydrodynamic conditions were also studied gravimetrically. The results from these studies imply that the new ternary inhibitor formulation, NTMP–Zn^{2+}–NA, is an effective, more environmentally friendly inhibitor of corrosion of carbon steel in cooling-water systems. Although gravimetric methods give more reliable information about loss of material during longer immersion under specified operating conditions [29], it is essential to consider other analytical techniques to understand the mechanism of corrosion inhibition by the new ternary inhibitor formulation. The objective of this investigation was to study the inhibition process by use of electrochemical techniques, viz., potentiodynamic polarization and impedance studies, and to analyse the protective surface film by surface analytical techniques, viz., XPS, FTIR spectroscopy, scanning electron microscopy (SEM), and atomic force microscopy (AFM). On the basis of all these studies, a plausible mechanism of corrosion inhibition is proposed.

Experimental

Materials

For all the surface analysis studies, specimens of dimensions 1.0 cm × 1.0 cm × 0.1 cm were taken from a single sheet of carbon steel of composition: C 0.1–0.2 %, P 0.04–0.07 %, S 0.03–0.04 %, Mn 0.3–0.5 %, and the remainder iron. Before the

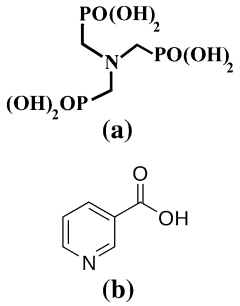

Fig. 1 Molecular structures of inhibitor components: **a** nitrilotris(methylenephosphonic acid (NTMP); **b** nicotinic acid (NA)

tests, the specimens were polished to a mirror finish with 1/0, 2/0, 3/0, and 4/0 emery polishing papers in sequence, washed with distilled water, degreased with acetone, and dried. The polished specimens were immersed, in duplicate, in 100 mL control solution in the absence and presence of the effective inhibitor formulation for a period of 7 days.

NTMP ($C_3H_{12}NO_9P_3$), zinc sulfate ($ZnSO_4{\cdot}7H_2O$), nicotinic acid ($C_6NH_5O_2$), and other reagents were AnalaR grade. Molecular structures of NTMP and nicotinic acid are shown in Fig. 1. All the solutions were prepared with triple-distilled water. An aqueous solution consisting of 200 ppm NaCl was used as the control throughout the study.

Electrochemical studies

The potentiodynamic polarization studies and electrochemical impedance spectroscopic (EIS) studies were performed by use of the Electrochemical Workstation model IM6e (Zahner-elektrik, Germany) and the experimental data were analysed by use of Thales software. The measurements were conducted (in accordance with ASTM specifications) in a conventional three-electrode cylindrical glass cell with platinum electrode as auxiliary electrode and Ag/AgCl (3 M KCl) as reference electrode. The working electrode was carbon steel embedded in polytetrafluoroethylene so that a flat surface of area 1 cm^2 was the only surface exposed to the electrolyte. The three-electrode system was immersed in control solution of volume 500 mL, both in the absence and presence of different inhibitor formulations, and left to attain a stable open circuit potential (OCP). Polarization curves were recorded in the potential range -1000 to $+200$ mV, with resolution of 2 mV. The curves were recorded in the dynamic scan mode with a scan rate of 2 mV s^{-1} in the current range -20 to $+20$ mA. The corrosion potential (E_{corr}), corrosion current density (I_{corr}), anodic Tafel slope (β_a), and cathodic Tafel slope (β_c) were obtained by extrapolation of anodic and cathodic regions of the Tafel plots. The inhibition efficiency (IE_p) values were calculated from I_{corr} values by use of the equation [30]:

$$\mathrm{IE_p}(\%) = \left[1 - \left(I'_{\mathrm{corr}}/I_{\mathrm{corr}}\right)\right] \times 100 \quad (1)$$

where I_{corr} and I'_{corr} are the corrosion current densities for control and inhibited solutions, respectively.

Electrochemical impedance spectra in the form of Nyquist plots were recorded at OCP in the frequency range 60 kHz to 10 mHz with 4–10 steps per decade. A sine wave, of amplitude 10 mV, was used to perturb the system. The impedance data, viz., charge transfer resistance (R_{ct}), constant phase element (CPE), and CPE exponent (n), were obtained from the Nyquist plots. The inhibition efficiencies ($\mathrm{IE_i}$) were calculated by use of the equation:

$$\mathrm{IE_i}(\%) = 100\left[1-\left(R_{\mathrm{ct}}/R'_{\mathrm{ct}}\right)\right] \quad (2)$$

where R_{ct} and R'_{ct} are, respectively, the charge-transfer resistance in the absence and presence of the inhibitor.

Surface analysis by X-ray photoelectron spectroscopy (XPS)

XPS measurements of the surface film were performed with a Kratos Analytical photoelectron spectrometer (AXIS 165) with a monochromated Al K_α X-ray source (1,486.6 eV). The spectra were collected at an electron take-off angle of 90°. Deconvolution spectra were recorded with analyser pass energy of 80 eV, with a step of 0.1 eV for the elements of interest. Binding energies for the deconvolution spectra were corrected individually for each set of measurements, on the basis of a value of 285.0 eV for the C–C component of C 1s.

Fourier-transform infrared (FTIR) spectroscopic studies

FTIR spectra were recorded by use of a Nexus 670 FTIR spectrophotometer from Thermo Electron Corporation, USA. The detector is temperature-stabilised DTGS (KBr window) and liquid nitrogen cooled MCT-A and the beam splitter is XT-KBr. FTIR spectra of pure NTMP and pure nicotinic acid were recorded by use of the KBr pellet method. The FTIR spectra of the surface films were recorded in the wavenumber range 4,000–400 $\mathrm{cm^{-1}}$. The measurements were made at a grazing angle of 85°.

Surface morphological and topographical studies

The surface morphology was observed by scanning electron microscopy (SEM), and topographical studies were conducted by atomic force microscopy (AFM). SEM images were recorded by use of an FEI Quanta FEG 200 high-resolution scanning electron microscope, at two different magnifications, for specimens immersed in the control and inhibitor solutions. AFM topographical images were obtained by use of a Dimension 3100 (Nanoscope-IV) atomic force microscope in contact mode with a commercial Si_3N_4 cantilever.

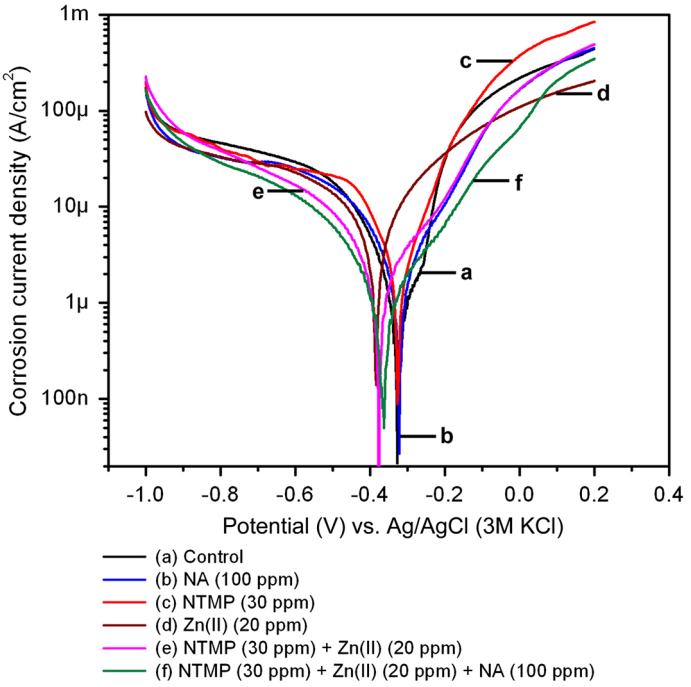

Fig. 2 Potentiodynamic polarization curves of carbon steel in different aqueous environments containing 200 ppm NaCl

Results and discussion

Potentiodynamic polarization studies

The potentiodynamic polarization curves for carbon steel electrodes in 200 ppm NaCl solution at pH 7 and 30 °C in the absence and presence of different inhibitor components are shown in Fig. 2. Tafel data derived from these curves, and inhibition efficiencies, are listed in Table 1. The corrosion potential (E_{corr}) for the control is −325.8 mV vs. Ag/AgCl (3 M KCl) and the corresponding corrosion current density (I_{corr}) is 12.33 µA cm^{-2}. NTMP alone shifts the E_{corr} value slightly to the more cathodic side. In the presence of NTMP (30 ppm) alone, the I_{corr} value is increased to 15.35 µA cm^{-2}. The shift in the anodic Tafel slope (β_a) is more than the shift in the cathodic Tafel slope (β_c) in the presence of NTMP (30 ppm) alone. When zinc ions alone are added to the control, the cathodic current densities are slightly reduced. The cathodic reaction is controlled by formation of zinc hydroxide at cathodic sites. The corrosion potential is shifted to the cathodic side and the shift in the anodic Tafel slope is slightly greater than the shift in the cathodic Tafel slope. Similar to the result obtained for NTMP, zinc ions increased the rate of corrosion, as inferred from the increase in the corrosion current density. Such an increase in the rate of corrosion in the presence of zinc ions alone has also been reported in the literature [31].

Table 1 Tafel data for carbon steel in 200 ppm NaCl solution in the absence and presence of different inhibitor components

Concentration (ppm)			Tafel data				Inhibition efficiency, IE_p (%)
NTMP	Zn^{2+}	NA	E_{corr} (mV) vs. Ag/AgCl (3 M KCl)	I_{corr} (μA cm^{-2})	β_a (mV dec^{-1})	β_c (mV dec^{-1})	
0	0	0	−325.8	12.33	234	711	–
30	0	0	−327.6	15.35	174	752	−24.49
0	20	0	−383.9	14.03	287	684	−13.78
0	0	100	−321.5	10.26	189	692	16.78
30	20	0	−377.1	4.94	192	467	59.93
30	20	100	−363.3	1.38	203	382	88.80

From the polarization curves shown in Fig. 2, it is clear that the combination of NTMP (30 ppm) and Zn^{2+} (20 ppm) substantially reduced both the anodic and cathodic current densities compared with the control. It is, thus, evident that this formulation acts as a mixed-type inhibitor. There is a shift of corrosion potential to the more cathodic side, and the shift of the cathodic Tafel slope is greater than the shift of the anodic Tafel slope. The corrosion current density is substantially reduced to 4.94 μA cm^{-2}, corresponding to an inhibition efficiency of 59.93 %.

When nicotinic acid alone is considered, the E_{corr} value is shifted slightly to anodic potential and the corrosion current density is slightly reduced to 10.26 μA cm^{-2}. The inhibition efficiency is found to be only 16.78 %, which is less than that obtained for the binary system containing NTMP and Zn^{2+}. It is interesting to note that the ternary formulation obtained by adding 100 ppm nicotinic acid to the binary system, NTMP (30 ppm)–Zn^{2+} (20 ppm) drastically reduced the corrosion current density to 1.38 μA cm^{-2}, corresponding to an inhibition efficiency of 88.80 %. This result is in agreement with the inhibition efficiency obtained from gravimetric studies [28] and clearly implies synergistic action of NTMP, Zn^{2+}, and nicotinic acid in control of the corrosion of carbon steel. In the presence of the ternary inhibitor formulation, both the cathodic and anodic current densities are substantially reduced. The corrosion potential is shifted to an extent of approximately 37.5 mV in the cathodic direction. It may also be noted that the shift in the cathodic Tafel slope is much higher than that in the anodic slope. All these results indicate that the ternary inhibitor formulation retards both anodic dissolution of carbon steel and oxygen reduction at cathodic sites in the corrosion-inhibition process. Nevertheless, the effect on cathodic reaction is more pronounced. Similar phosphonate-based formulations have been reported to be mixed inhibitors [5, 21, 32].

Electrochemical impedance studies

Nyquist plots for carbon steel immersed in 200 ppm NaCl solution at pH 7 in the absence and presence of different formulations are shown in Fig. 3. For the control and the different formulations, the Nyquist plots are found to be depressed

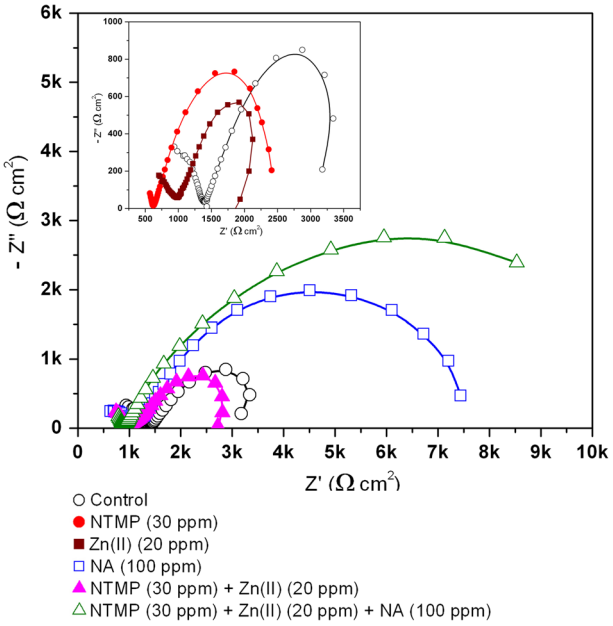

Fig. 3 Nyquist plots for carbon steel in 200 ppm NaCl and in different inhibitor components (*lines* represent fitted curves)

semicircles instead of ideal semicircles. All the Nyquist plots obtained in this study are characterized by two time constants. The experimental data obtained from these plots are fitted by the equivalent electrical circuit shown in Fig. 4. Such an equivalent circuit has also been discussed by other researchers [33, 34], who obtained similar Nyquist plots. The impedance data, viz., charge transfer resistance (R_{ct}), film resistance (R_f), constant phase element of the double layer (CPE_{dl}), constant phase element of the film (CPE_f), CPE exponent values of the double layer and the film obtained from the Nyquist plots, and the calculated inhibition efficiency (IE_i) values are listed in Table 2.

In the presence of the control alone, two small semicircles were observed, one corresponding to the metal–film interface and the other to the film–solution interface. The R_{ct} and R_f values are 2.232 and 1.332 kΩ, respectively. Similar semicircles are also obtained when 20 ppm of Zn^{2+} is added to the control. Because of the Zn^{2+} ions, the R_{ct} and R_f are reduced. The CPE of the double layer is slightly reduced whereas that of the film is increased. These changes are because of replacement of water molecules in the interfaces by the zinc ions, which resulted in an increased rate of corrosion. On addition of 30 ppm NTMP to the control, two slightly depressed semicircles are formed. One is in the higher-frequency region and the other, large, semicircle is towards the lower-frequency region. Both R_{ct} and R_f values are reduced. The CPE of both the double layer and the film are slightly increased. These observations can be attributed to the presence of organic inhibitor molecules in the double layer. When the combination of 30 ppm NTMP and 20 ppm

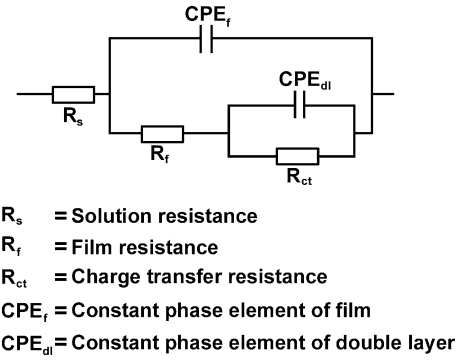

Fig. 4 Equivalent circuit used to calculate the impedance data

Table 2 Impedance data for carbon steel in 200 ppm NaCl in the absence and presence of inhibitor formulations

Concentration (ppm)			Impedance data						Inhibition efficiency, IE_i (%)
NTMP	Zn^{2+}	NA	R_{ct} (kΩ cm^2)	$(CPE)_{dl}$ (μF cm^{-2})	n	R_{film} (kΩ cm^2)	$(CPE)_{film}$ (nF cm^{-2})	n_{film}	
0	0	0	2.232	71.08	0.732	1.332	5.896	0.624	–
30	0	0	1.993	85.96	0.710	0.455	6.494	0.651	−11.99
0	20	0	1.329	67.23	0.611	0.969	15.93	0.447	−67.94
0	0	100	6.824	7.473	0.653	0.848	9.324	0.657	67.29
30	20	0	2.361	13.60	0.602	0.784	16.54	0.666	5.46
30	20	100	11.84	5.79	0.879	1.753	2.939	0.852	81.15

Zn^{2+} is considered in the presence of control, there is a slight increase in charge-transfer resistance and film resistance. The CPE of the double layer is reduced and the CPE of the film is increased. The inhibition efficiency of the NTMP–Zn^{2+} combination is only 5.46 %. When 100 ppm nicotinic acid alone is used, the R_{ct} value is increased to 6.824 kΩ, corresponding to an inhibition efficiency of 67.29 %, which is much higher than that obtained by use of the binary inhibitor system containing NTMP and Zn^{2+}. As expected, the CPE of the double layer is reduced.

When 100 ppm nicotinic acid is added to 30 ppm of NTMP and 20 ppm of Zn^{2+}, a large depressed capacitive loop related to the double layer is observed. This semicircle represents an R_{ct} value of 11.84 kΩ, which is approximately five times greater than that observed for the control. The CPE_{dl} at the interface is found to decrease from 71.08 μF cm^{-2} for the control to 5.79 μF cm^{-2} for the ternary inhibitor formulation. This is because of replacement of water molecules in the electrical double layer by the organic molecules with low dielectric constants [35].

The value of n is substantially increased, to 0.879, in the presence of the ternary inhibitor system, suggesting increased homogeneity of the interface during inhibition. These results are indicative of formation of a protective film in the

presence of the ternary inhibitor formulation. The film resistance is found to be 1.753 kΩ. This value is higher than that in the absence of any inhibitor. The chemical composition of the film at the interface may be entirely different in the presence of the inhibitor formulation. This inference is supported by the expected changes in the other impedance data, viz., R_{ct}, CPE_{dl}, CPE_f, and n values. Several authors who studied the inhibitory effects of phosphonate-based corrosion inhibitors also reported the formation of a thick and less permeable protective film on the metal surface [3, 5, 21]. The impedance results in our study also imply synergistic action among NTMP, Zn^{2+}, and nicotinic acid. This is in agreement with the inferences drawn from gravimetric studies [28] and polarization studies.

Nyquist plots for carbon steel in the control and in the inhibitor formulation NTMP (30 ppm) + Zn^{2+} (20 ppm) + nicotinic acid (100 ppm) for different immersion periods (1–24 h) and at constant temperature (30 °C) are shown in Fig. 5. Impedance data obtained from these plots and the inhibition efficiencies calculated from the R_{ct} values are listed in Table 3. All the Nyquist plots are depressed capacitive loops, which are characterized by two time constants. For the control, there is a decrease in both R_{ct} and R_f with immersion period, whereas the non-ideal capacitance values increase. The CPE exponent values are found to be less after an immersion period of 24 h compared with immersion for 1 h. The significant increase in CPE is because of a large increase in the specific area caused by the presence of corrosion products on the metallic surface with time [36]. For the inhibitor formulation, there is an increase in R_{ct} value and a decrease in CPE_{dl} with increasing immersion time. The decrease in CPE_{dl} may be because of continuous displacement of the hydrated layer at the double layer by the developing inhibitor film on the surface [37]. Supposing that the electrochemical processes are occurring only at the pores and pinholes of the surface film, the increasing R_{ct} values give direct information on the growth and quality of the inhibitor film. Thus, these observations indicate that a continuous build-up of inhibitor film is occurring with time, resulting in the formation of a protective layer at the surface.

For the inhibitor formulation, the values of n for different immersion periods are closer to 0.9, which implies that the homogeneity of the surface film is maintained during the immersion period studied. The inhibitor film formed after an immersion period of 24 h by all three components of the inhibitor formulation resulted in the rapid fall in the rate of iron dissolution, as indicated by its highest inhibition efficiency of 95.53 %. From these studies, it may be noted that this highest inhibition efficiency, achieved after an immersion time of 24 h, is close to that obtained by gravimetric measurements [28]. It is, therefore, inferred that an immersion time of 24 h is required for formation of the protective film over the entire surface.

A significant observation related to the inhibition efficiency must be noted. If the inhibition efficiencies obtained from gravimetric (IE_g) [28], polarization (IE_p), and EIS (IE_i) studies are compared, slight differences are observed. It is suggested that the IE values obtained from the different methods may not be strictly compared, because the immersion times considered for all these methods are not the same.

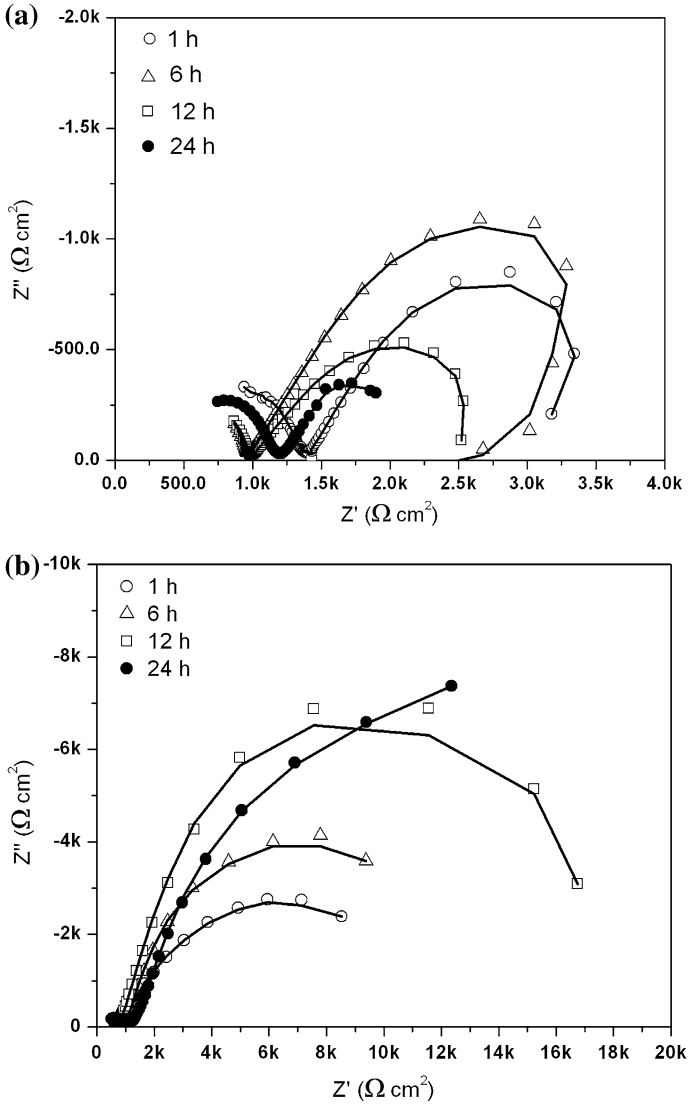

Fig. 5 Nyquist plots for carbon steel, in the absence **a** and presence **b** of inhibitor, for different immersion periods

X-ray photoelectron spectroscopic studies (XPS)

The XPS survey spectra of the surface films formed on carbon steel in the absence and presence of the inhibitor system NTMP (30 ppm) + Zn^{2+} (20 ppm) + nicotinic acid (100 ppm) are shown in Fig. 6. The XPS deconvolution spectra of the individual elements present in these surface films are shown in Figs. 7, 8, 9, 10, 11, and 12. These spectra are interpreted with the help of elemental binding energies

Table 3 Impedance data for carbon steel in 200 ppm NaCl in the absence and presence of the inhibitor formulation for different immersion periods and at a constant temperature of 30 °C

Immersion period (h)	Impedance data						Inhibition efficiency (%)
	R_{ct} (kΩ cm^2)	CPE (μF cm^{-2})	n	R_{film} (kΩ cm^2)	$(CPE)_{film}$ (nF cm^{-2})	n_{film}	
Control (200 ppm NaCl)							
1	2.232	71.08	0.732	1.332	5.896	0.624	–
6	2.006	75.14	0.714	1.347	6.948	0.636	–
12	1.781	74.55	0.671	1.188	5.358	0.676	–
24	1.314	87.03	0.614	0.924	7.839	0.587	–
Inhibitor formulation—NTMP (30 ppm) + Zn^{2+} (20 ppm) + NA (100 ppm)							
1	11.84	5.79	0.879	1.753	2.939	0.852	81.15
6	16.06	4.17	0.863	1.956	2.484	0.815	87.51
12	19.03	3.27	0.884	1.693	2.356	0.862	90.64
24	29.43	3.74	0.849	1.457	2.107	0.818	95.53

reported in literature and with the help of the reports published on analysis of XPS spectra of the surface films.

The Fe 2p deconvolution spectrum for the control is shown in Fig. 7a. Two peaks are observed, one at 711.6 eV, corresponding to Fe $2p_{3/2}$, and the other at 725.1 eV, corresponding to Fe $2p_{1/2}$. The Fe $2p_{3/2}$ peak is interpreted for determination of the chemical state of iron in the surface film. The Fe $2p_{3/2}$ peak at 711.6 eV is shifted from 707.0 eV, the characteristic elemental binding energy of the Fe $2p_{3/2}$ electron [38]. Such a large shift of 4.6 eV suggests that iron is present in the Fe^{3+} state in the surface film. This peak can be ascribed to the presence of iron in the form of γ-Fe_2O_3, Fe_3O_4, and α-FeOOH in the surface film [5, 39–41]. The spectrum shown in Fig. 7b corresponds to the Fe $2p_{3/2}$ peak in the presence of the inhibitor system. It shows a peak at 711.4 eV. This peak implies the presence of oxides and hydroxides, for example γ-Fe_2O_3, Fe_3O_4, and α-FeOOH, and involvement of Fe^{3+} in the complex formed with the inhibitor molecules. No peak from elemental iron is observed for either the control or the inhibitor formulation. This result implies the formation of thick films in both cases. The film is non-protective in the control and highly protective in the presence of inhibitor molecules. If the intensities of the Fe $2p_{3/2}$ peaks are compared, they are 16,000 cps for the control and only 6,000 cps for the inhibitor system. Such a drastic decrease in the intensity of the Fe 2p peak in the presence of the inhibitor formulation is because of formation of a protective film, and, as a consequence, less corrosion of iron and less of iron oxide. The binding energy of the Fe^{2+} state in iron oxides is reported in the literature to be approximately 708.5 eV [42]. The absence of any peak in this region in our study also suggests that iron does not exist in the Fe^{2+} state.

The XPS spectrum of phosphorus in the surface film formed by the inhibitor formulation is shown in Fig. 8. Two P 2p peaks are observed, one at 133.0 eV and the other at 134.3 eV. In the literature [43], it has been reported that the P 2p peak

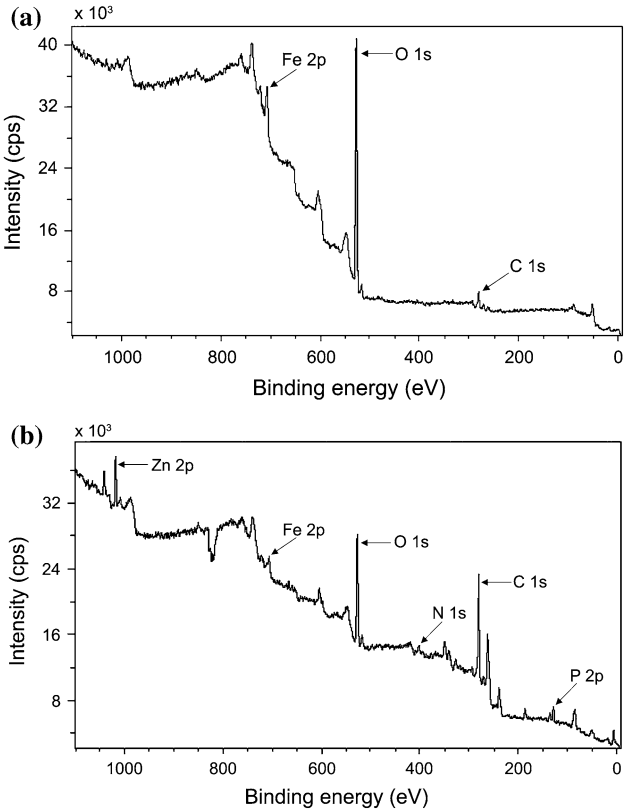

Fig. 6 XPS survey spectra of the surface films formed on carbon steel in the absence and presence of inhibitor system: **a** control; **b** inhibitor formulation

could be observed in the range 132.9–133.8 eV for iron or steels immersed in solutions containing phosphonates, orthophosphates, or polyphosphates. Nakayama obtained a P 2p peak at 133.0 eV and attributed it to the presence of phosphonate compounds [22]. Ochoa et al. [9] in their studies on mixtures of salts of phosphonocarboxylic acids and fatty amines as inhibitors of corrosion of carbon steel reported the P 2p peak at 132.1 eV and interpreted on the basis of the presence of the phosphonate group in the surface film. In the light of these reports, the P 2p peaks observed in this present study suggest the presence of NTMP in the surface film, probably in the form of a complex with the metal ions Fe^{3+} and Zn^{2+}.

Figure 9 shows the XPS deconvolution spectrum of N 1s. It contains two peaks, one at 398.6 eV and another at 400.3 eV, and the characteristic elemental binding energy of the N 1s electron is 398.0 eV [38]. This shift of binding energy may be attributed to the presence of NTMP and nicotinic acid species in the surface film in the form of a complex with Fe(III) and Zn(II). It has been reported [44] that the N 1s peak observed at 399.7 eV could be assigned to the presence of (=N–) in the molecule adsorbed on the metal surface. Meneguzzi et al. [45] reported the N 1s

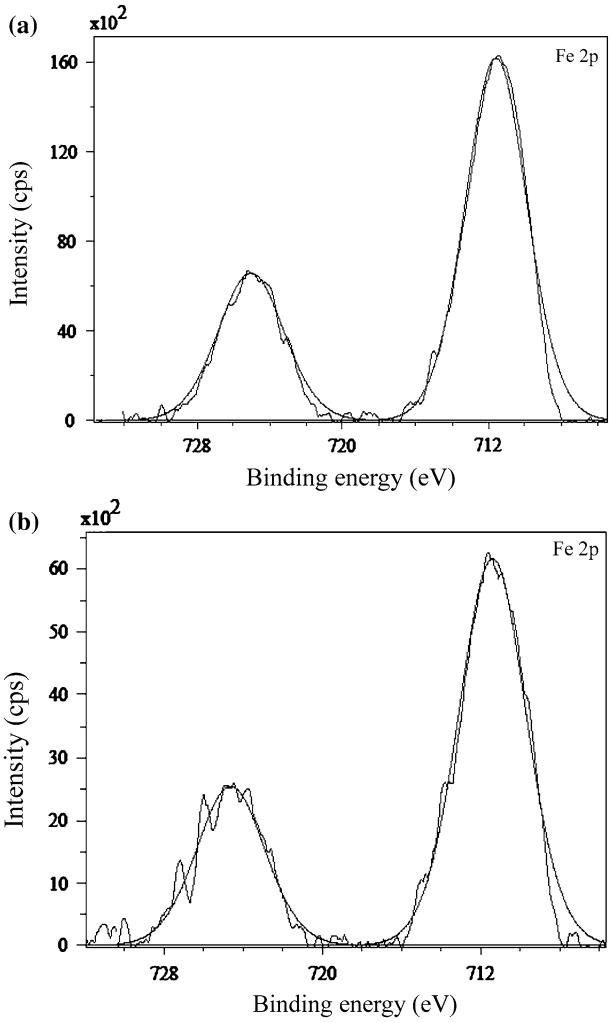

Fig. 7 XPS deconvolution spectra of Fe 2p in the surface films formed on carbon steel in the absence and presence of inhibitor system: **a** control, **b** inhibitor formulation

peak at 399.9 eV and assigned it to the neutral imine (–N=) and amine (–N–H) nitrogen atoms. The XPS spectra of C 1s are shown in Fig. 10. The C 1s spectrum for the control (Fig. 10a) contains a single peak at 284.9 eV. This peak is because of contamination from the vacuum system and chamber during the analysis [46]. For the inhibitor formulation, the C 1s spectrum (Fig. 10b) contains three peaks, one of which is the high-intensity peak at 284.6 eV and the other two are low intensity peaks at 286.1 and 287.9 eV. Reports in the literature [6, 9, 47, 48] imply that the three peaks observed in this study also arise because of the presence of both NTMP and nicotinic acid in the surface film.

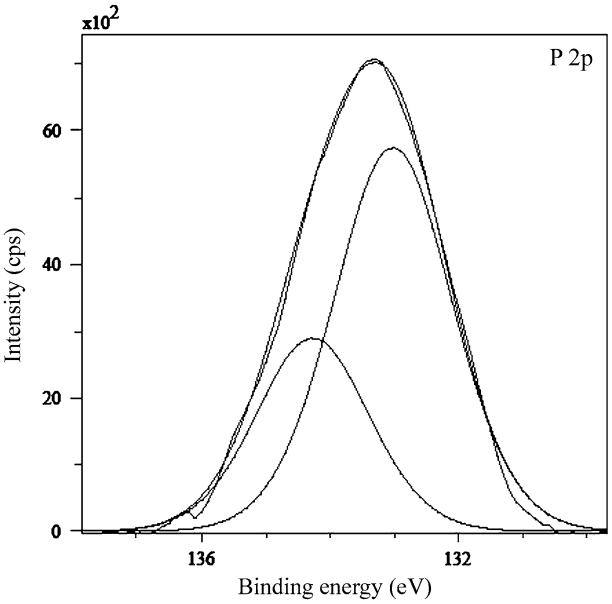

Fig. 8 XPS deconvolution spectrum of P 2p in the surface film formed on carbon steel in the presence of the inhibitor formulation

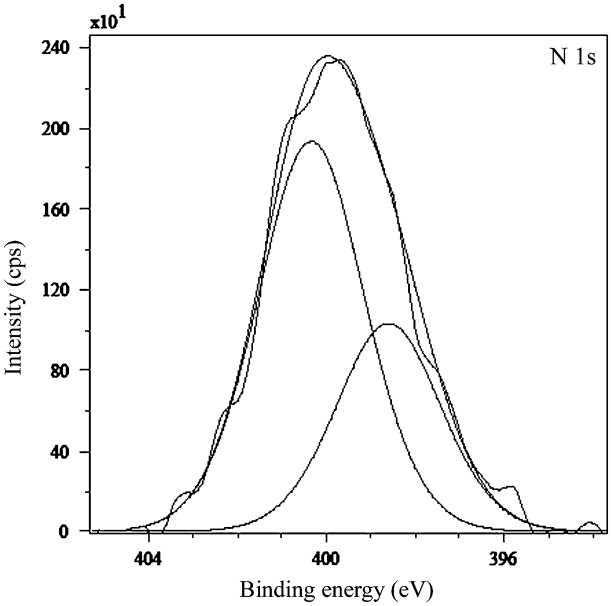

Fig. 9 XPS deconvolution spectrum of N 1s in the surface film formed on carbon steel in the presence of the inhibitor formulation

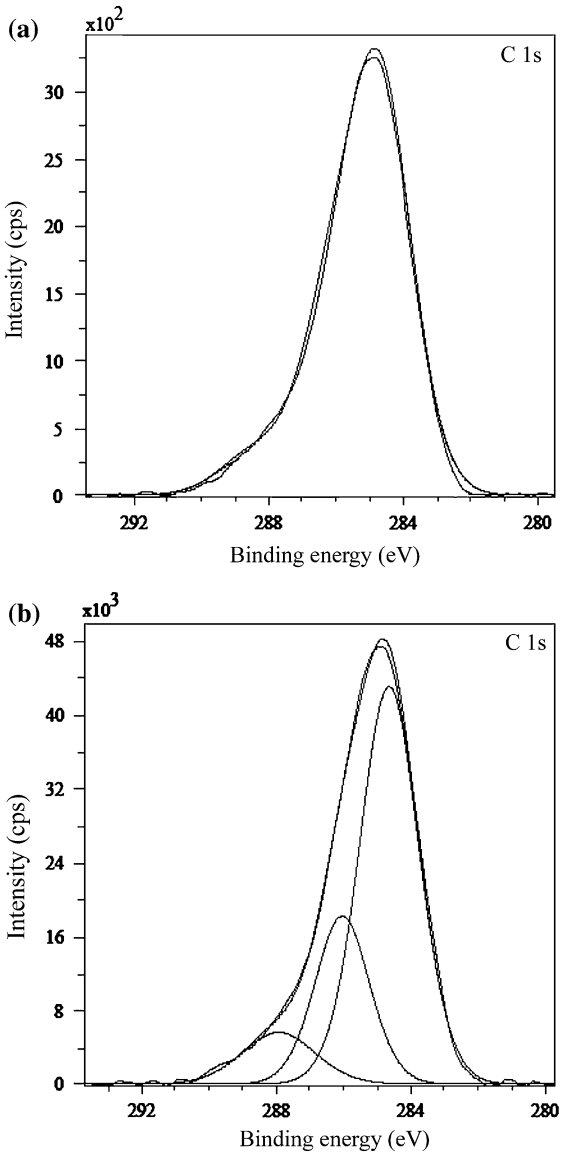

Fig. 10 XPS deconvolution spectra of C 1s in the surface films formed on carbon steel in the absence and presence of the inhibitor system: **a** control; **b** inhibitor formulation

The XPS spectra of O 1s are presented in Fig. 11. For the control (Fig. 11a), two peaks corresponding to O 1s are observed, one at 531.6 eV and the other at 533.0 eV. The latter peak is essentially because of water adsorbed on the metal surface [9, 22, 42, 49]. In this study the O 1s peak at 531.6 eV is because of O^{2-} [5, 49]. The presence of O^{2-} in the surface film formed on the control may be in the form of oxides and/or hydroxides of Fe(III). For the inhibitor formulation, two O 1s peaks are observed. They are located at 531.1 and 532.5 eV. Fang et al. [23] ascribed the O 1s peak at 531.3 eV to the complex formed between iron and

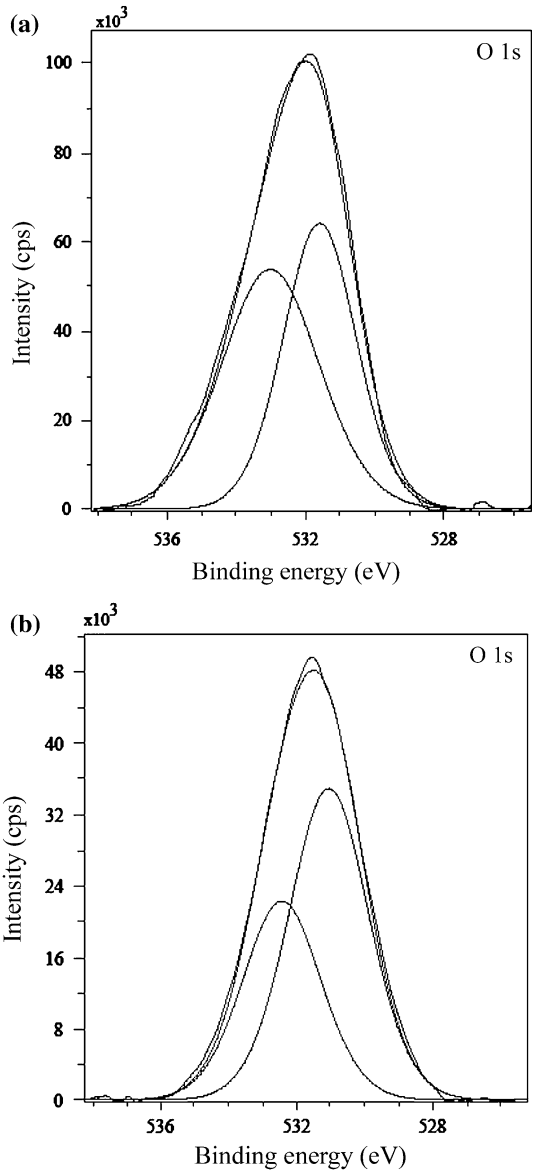

Fig. 11 XPS deconvolution spectra of O 1s in the surface films formed on carbon steel in the absence and presence of the inhibitor system: **a** control, **b** inhibitor formulation

phosphonate. Pech-Canul and Bartolo-Perez [5] observed the O 1s peak at 531.3 eV, which was ascribed to OH^- from hydrous iron oxides and to the complex formed between iron and the phosphonate group. It was also mentioned in their paper that such hydrous ferric oxides consist of $Fe(OH)_3$ and FeOOH. In the light of these results, the O 1s peaks of high intensity observed in this study may be interpreted as follows. XPS of the surface films (Fig. 6) shows that, besides oxygen, carbon, phosphorus, nitrogen, iron, and zinc are present in the surface film. That

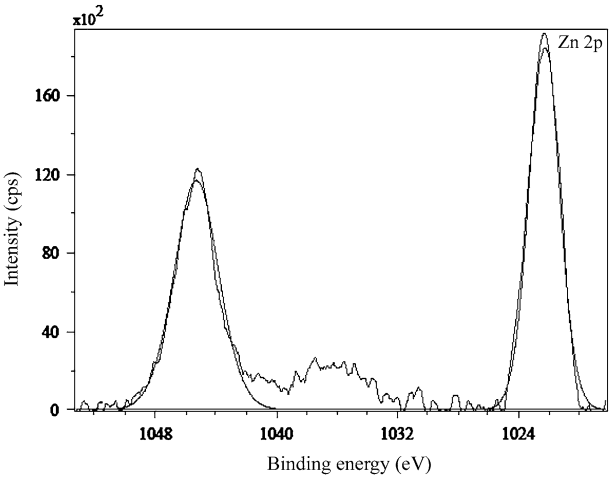

Fig. 12 XPS deconvolution spectrum of Zn 2p in the surface film formed on carbon steel in the presence of the inhibitor formulation

means NTMP and nicotinic acid are present on the surface, zinc is present as Zn^{2+}, and the interpretation given above for Fe 2p indicates the presence of γ-Fe_2O_3, Fe_3O_4, and α-FeOOH. Hence, O 1s peaks can be ascribed to the presence of $Zn(OH)_2$, γ-Fe_2O_3, Fe_3O_4, α-FeOOH, and oxygen of NTMP and nicotinic acid in the surface film. The absence of any peak at 533.0 eV for the inhibitor formulation indicates the absence of water molecules in the surface film.

Figure 12 is the XPS deconvolution spectrum of zinc present in the surface film formed by the inhibitor formulation. The Zn $2p_{3/2}$ peak is observed at 1022.3 eV and the Zn $2p_{1/2}$ peak at 1045.3 eV. The high intensities of the Zn $2p_{3/2}$ peaks may be ascribed to the presence of $Zn(OH)_2$ in the surface film and to involvement of Zn^{2+} in complex formation with NTMP and nicotinic acid [3]. After consolidating all the inferences drawn from the XPS of individual elements present in surface films, it is suggested that the surface film formed by the inhibitor formulation consists of mainly of the Zn(II)–NTMP–nicotinic acid complex, $Zn(OH)_2$, and small amounts of oxides and/or hydroxides of Fe(III). The complex may be chemisorbed on the metal surface and become attached to Fe(III) ions.

Surface analysis by FTIR spectroscopy

The FTIR spectra of the surface films formed on carbon steel in the absence and presence of the inhibitor formulation are shown in Figs. 13 and 14, respectively. The spectrum obtained from the inhibited surface was interpreted by comparison with the FTIR spectra of pure NTMP and nicotinic acid (not included here) and with the help of literature reports. In the FTIR spectrum of pure NTMP, multiple bands in the region, 900–1,270 cm^{-1} can be assigned to $-PO_3$ stretching frequencies. The band at 1,002 cm^{-1} is assigned to P=O stretching and the band at 1,145 cm^{-1} is assigned to C–N stretching [23]. The O–H stretching is observed as a broad band at

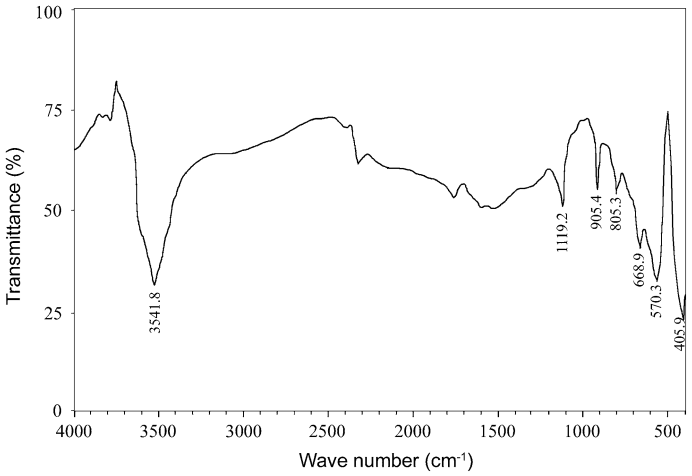

Fig. 13 FTIR spectrum obtained from the film on the surface of carbon steel placed in control solution in the absence of the inhibitor formulation

3,260 cm^{-1}. In the spectrum obtained from the inhibited surface film formed by the inhibitor formulation, the P=O peak is shifted from 1,002 to 1,032 cm^{-1}. The P–OH stretching located at 930 cm^{-1} for pure NTMP is not observed in the FTIR spectrum obtained from the surface film. These results can be interpreted in terms of interaction between $P–O^-$ present in the phosphonate with metallic species, viz., Zn(II) and Fe(III), to form P–O–Zn and P–O–Fe bonds. This interpretation is in accord with that of several authors who worked on inhibition of corrosion of carbon steel by phosphonates [21, 50, 51]. Carter et al. [52] found that the FTIR spectra obtained from an organic phosphonate on a steel substrate are consistent with reaction of the phosphonate with steel to produce a metal salt. It also suggests that phosphonates are coordinated with metal ions, resulting in the formation of metal–phosphonate complexes on the metal surface.

A weak band observed in the spectrum (Fig. 14) at approximately 1,336 cm^{-1} indicates the presence of zinc hydroxide in the surface film [10, 51, 53]. The intense band assigned to asymmetric stretching vibrations of –COOH in pure nicotinic acid is observed at 1,708 cm^{-1}; the band assigned to symmetric stretching is at 1,350 cm^{-1}. Uncoordinated nicotinic acid gave a strong peak at 1,460 cm^{-1}, which is characteristic of the imine C–N group. When the inhibitor formulation is used, the C=O stretching frequency is observed as an absorption band at 1,636 cm^{-1}. The band at 2,924 cm^{-1} in the FTIR spectrum of the surface film is indicative of C–H stretching of nicotinic acid. The presence of these bands in the spectrum obtained from the surface film is indicative of the presence of inhibitor molecules, viz., NTMP and nicotinic acid, in the surface film. The shifts of the stretching frequencies of functional groups present in the inhibitor molecules are a result of involvement of these molecules in complex formation.

Several bands in the region 1,200–400 cm^{-1} in the spectrum obtained from the surface film formed in the control alone (Fig. 13) are not observed when the

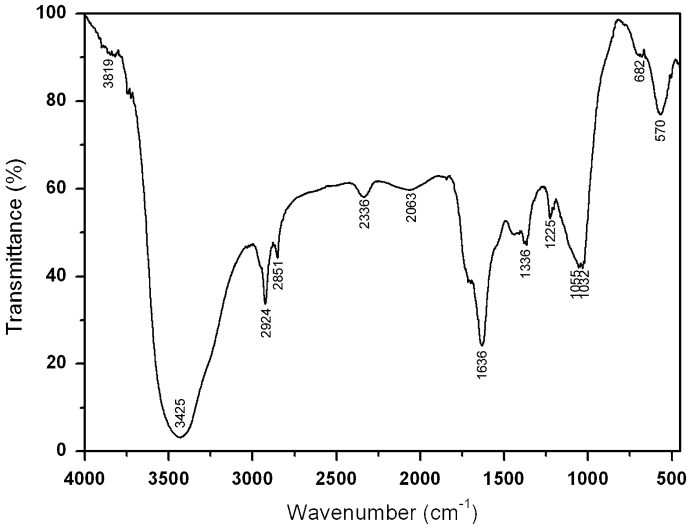

Fig. 14 FTIR spectrum obtained from the film on the surface of carbon steel placed in solution containing the inhibitor formulation, NTMP (30 ppm) + Zn^{2+} (20 ppm) + nicotinic acid (100 ppm)

inhibitor formulation is used. Many of these peaks imply the presence of a variety of oxides and hydroxides of iron, for example Fe_3O_4, α-FeOOH, and γ-Fe_2O_3 [22, 48, 51, 54]. A moderately intense and a broad band observed at 3,541.8 cm^{-1} for the control can be assigned to the presence of –OH groups on the surface. These hydroxyl groups may be in the form of FeOOH and/or $Fe(OH)_3$ [55]. The broad and intense band at 3,425 cm^{-1} is also contributed by the –OH groups present in NTMP, $Zn(OH)_2$ and possibly traces of ferric hydroxide present in the inhibited film. Thus, the FTIR spectrum obtained from the surface film formed in presence of the inhibitor formulation implies the presence of Zn(II)–NTMP–nicotinic acid complex, $Zn(OH)_2$, and small amounts of oxides and hydroxides of Fe(III).

The XPS and the FTIR spectra of the inhibited surface film imply the presence of Fe(III), Zn(II), NTMP, and nicotinic acid in the surface film. The shifts in binding energies of the different elements, and shifts in the absorption band frequencies of the different functional groups imply that NTMP and nicotinic acid are involved in complex formation with Zn^{2+} and Fe^{3+}. This inference is further supported by several studies reported in the literature [21, 56–58]. Papadaki and Demadis [59] synthesised metal phosphonate organic–inorganic polymeric hybrid materials, characterised them, and studied their anticorrosion properties for protection of carbon steels. They inferred formation of metal phosphonate complexes on the metal surface when the surface is in contact with solution containing phosphonate and such metal ions as Zn^{2+}, Ca^{2+}, Ba^{2+}, Sr^{2+}, etc. They also concluded that protection efficiency of such formulations depends on the structure of metal phosphonate complex formed on the carbon steel surface and on the formation constant of the complex. In another study by Demadis et al. [60], the complexes of hexamethylenediaminetetrakis(methylenephosphonate) (HDTMP) with Zn^{2+} and

Ca^{2+} were prepared and the crystal structures of Zn–HDTMP and Ca–HDTMP were determined by use of X-ray diffraction and FTIR spectroscopy. Similar significant studies performed Demadis and coworkers [61–65] have been reported in the literature. These investigations were conducted to characterise metal–phosphonate systems and to discover how such hybrid systems made the surface films protective. They also studied the relationship between the chemical structures of metal phosphonates and their efficiency in corrosion inhibition.

On the basis of all these literature reports on different phosphonates, the requirement of an optimum concentration of zinc ions for effective inhibition, and the high intensity Zn 2p peaks in XPS spectra, it can be inferred that Zn(II) and Fe(III) react with NTMP and nicotinic acid to form Fe(III), Zn(II)–NTMP–nicotinic acid polynuclear multiligand complexes which are crucially involved in making the surface film protective.

Study of surface morphology by scanning electron microscopy (SEM)

Figure 15 shows high-resolution SEM images of the surfaces of carbon steel immersed for seven days in the control solution in the absence and presence of the inhibitor formulation, NTMP (30 ppm) + Zn^{2+} (20 ppm) + nicotinic acid (100 ppm). Figure 15a reveals the surface is severely corroded; different corrosion products (iron oxides) are formed on the surface in the absence of any inhibitor. Morphological features of the inhibited surface are shown in Fig. 15b. The corrosion product deposits observed for the control surface are not present on the inhibited surface. This indicates that penetration of chloride ions from the environment into the substrate is controlled effectively by good surface coverage by the inhibitor film. The image corresponding to the inhibited surface is indicative of the presence of low-depth inhomogeneities on the surface. Closer study of such sites reveals the inhomogeneities are the result of structural defects of the metal substrate and that these sites are also covered by the inhibitor film. Thus, the inhibitor film covers the entire metal surface. This observation also explains the high values of the inhibition efficiency obtained during the gravimetric [28] and electrochemical studies of the inhibitor system. From the SEM analysis it can be inferred that the inhibitor film has good protective properties for carbon steel in a low-chloride environment.

Study of surface topography by atomic force microscopy (AFM)

Figure 16 shows AFM topographical images of the surfaces of carbon steel immersed for seven days in the control solution in the absence and presence of the inhibitor formulation, NTMP (30 ppm) + Zn^{2+} (20 ppm) + nicotinic acid (100 ppm). Severely corroded surface topography (Fig. 16a) with high surface roughness is observed after immersion in the control in the absence of the inhibitor. The microstructure of the surface is indicative of several deposits, both small and large, of corrosion products. In the presence of the inhibitor formulation, the surface topography is found to be homogeneous (Fig. 16b). The significant decrease in roughness when the inhibitor system is used implies homogeneity of the surface film

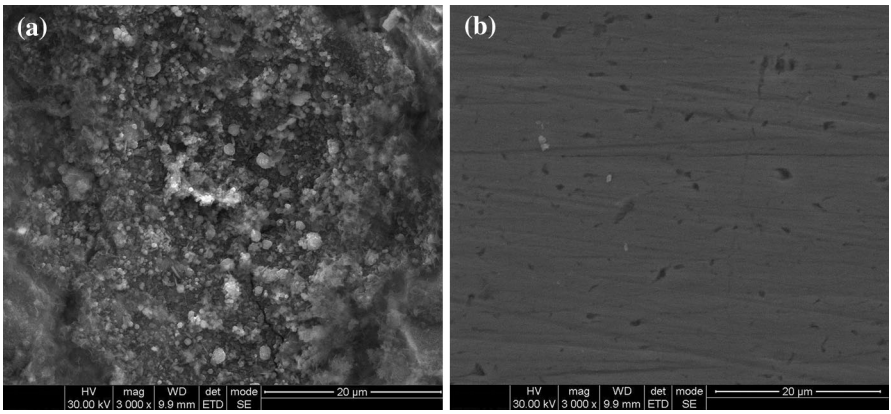

Fig. 15 High-resolution SEM images of carbon steel surfaces after immersion in the control solution in the absence and presence of the inhibitor system: **a** control; **b** NTMP (30 ppm) + Zn^{2+} (20 ppm) + nicotinic acid (100 ppm)

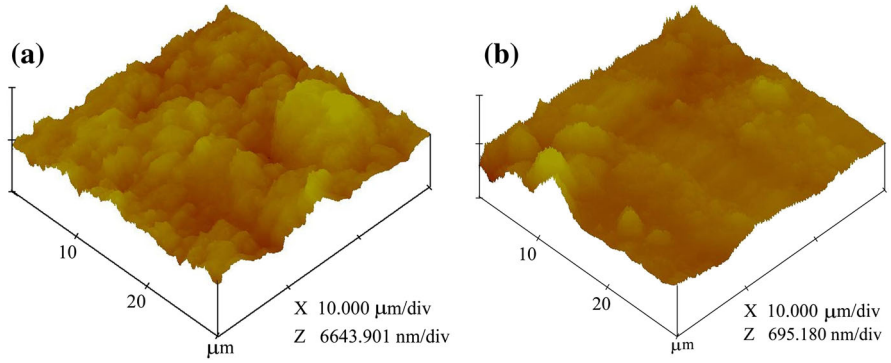

Fig. 16 AFM topographical images of carbon steel surfaces after immersion in the control solution in the absence and presence of the inhibitor system: **a** control, **b** NTMP (30 ppm) + Zn^{2+} (20 ppm) + nicotinic acid (100 ppm)

produced by the inhibitor formulation and the absence of corrosion product deposits. The results from surface topographical studies strongly support the inferences drawn above in the electrochemical studies, i.e. the protective nature of the surface film produced by the inhibitor formulation.

Mechanism of corrosion inhibition

To explain all the experimental results, a plausible mechanism of corrosion inhibition is proposed as follows.

1. The mechanism of corrosion of carbon steel in nearly neutral aqueous medium is well established. The well-known reactions are:

$$Fe \rightarrow Fe^{2+} + 2e^{-}$$

Fe^{2+} further undergoes oxidation in the presence of oxygen available in the aqueous solution:

$$Fe^{2+} \xrightarrow{[O_2]} Fe^{3+} + e^{-}$$

The corresponding reduction reaction at cathodic sites in neutral and alkaline media is:

$$O_2 + 2H_2O + 4e^{-} \rightarrow 4\ OH^{-}$$

Fe^{3+} ions produced in anodic areas and OH^{-} ions produced in cathodic areas combine to form $Fe(OH)_3$ (more correctly $Fe_2O_3{\cdot}H_2O$) which is precipitated on the surface of the metal because of its very low solubility product.

2. When NTMP, Zn^{2+}, and nicotinic acid (NA) are added to the aqueous solution, NTMP and NA react with Zn^{2+} to form a multiligand complex Zn^{2+}–NTMP–NA. This diffuses to the metal surface and binds to Fe(III) ions present on the surface. Cross-linking and reorganization of such complex ions on the surface will produce a polymeric network structure. The resulting polynuclear complex, Fe(III), Zn(II)–NTMP–NA covers the anodic sites and controls the corresponding anodic reaction. Formation of the protective layer by the phosphonate consists of a fast adsorption step and subsequent slower process, which is supposed to be a result of the reorganization. This effect is because of the formation of self-assembling layer of complexes of the organic inhibitor with iron [66].

$$[Zn(II) - NTMP - NA] + Fe^{3+} \rightarrow [Fe(III),\ Zn(II) - NTMP - NA]$$

3. Free Zn^{2+} ions are available in the bulk of the solution because of relatively higher molar concentration of Zn^{2+} in the inhibitor mixture. These Zn^{2+} ions diffuse to the metal surface and react with OH^{-} ions produced at the cathodic sites to form a precipitate of $Zn(OH)_2$. The precipitate of $Zn(OH)_2$ is deposited on the cathodic sites and controls the cathodic partial reaction of the corrosion process.

$$Zn^{2+} + 2OH^{-} \rightarrow Zn(OH)_2$$

4. The decrease in inhibition efficiency when the bulk concentration of nicotinic acid is higher than the optimum [28] can be explained as follows. When the bulk concentration of nicotinic acid is higher than that of NTMP, the nature and composition of the complex Zn(II)–NTMP–NA may be entirely different, with

more NA than NTMP. Such a complex may not be protective. Second, more NA is available in free form in the bulk of the solution. This free NA diffuses to the steel surface and is chemisorbed by the metal surface. As a result, the protective Zn(II)–NTMP–NA complex will not be available on the metal surface. It must be noted that NA alone does not afford significant inhibition.

5. The inhibitor formulation is effective in the pH range 5–9 [28]. At pH 10, higher concentrations of OH^- ions are available both in the bulk of the solution and on the surface. In such an environment, there is greater interference of OH^- ions with complexation [67] leading to formation of the complex Zn(II)–NTMP–NA–OH, which may not contribute to formation of a protective film on the metal surface. In acidic medium at pH 4, the ligands will be in the protonated form [68] and do not coordinate with Zn(II) as effectively as the deprotonated ligands. Second, sufficient $Zn(OH)_2$ will not be formed on the cathodic sites. Hence, the observed decrease in inhibition efficiency at pH 4.
6. Thus, NTMP, Zn^{2+}, and nicotinic acid are very important in the synergistic effect in controlling corrosion by formation of a protective film on the metal surface. It is inferred that the film may consist of a variety of oxides and/or hydroxides, for example γ-Fe_2O_3, $Fe_3O_4.H_2O$, and α-FeOOH, in trace quantities, $Zn(OH)_2$, and a polynuclear multiligand complex Fe(III), Zn(II)–NTMP–nicotinic acid. Each of these constituents contributes to making the film highly protective.

Conclusions

1. The effective and environmentally friendly corrosion inhibitor formulation NTMP–Zn(II)–NA is a mixed type inhibitor which controls both the anodic and cathodic partial reactions of corrosion of carbon steel.
2. In the presence of the ternary inhibitor formulation, there is significant modification of metal–solution interface, leading to formation of a protective surface film.
3. The time required to produce a protective film on most of the metal surface is 24 h. The film is uniform and continuous with relatively low roughness.
4. The film consists mainly of the polynuclear multiligand complex Fe(III), Zn(II)–NTMP–NA and $Zn(OH)_2$ with smaller quantities of oxides and/or hydroxides of iron.

Acknowledgments The authors based on V. R. Siddhartha Engineering College (Autonomous) are thankful to the Principal and Management of the Institute for their continuous encouragement in research activities.

References

1. H. Amar, J. Benzakour, A. Derja, D. Villemin, B. Moreau, J. Electroanal. Chem. **558**, 131 (2003)
2. H.S. Awad, S. Turgoose, Corrosion **60**, 1168 (2004)

3. I. Felhosi, Zs Keresztes, F.H. Karman, M. Mohai, I. Bertoti, E. Kalman, J. Electrochem. Soc. **146**, 961 (1999)
4. M.A. Pech-Canul, L.P. Chi-Canul, Corrosion **55**, 948 (1999)
5. M.A. Pech-Canul, P. Bartolo-Perez, Surf. Coat. Technol. **184**, 133 (2004)
6. L.Y. Reznik, L. Sathler, M.J.B. Cardoso, M.G. Albuquerque, Mater. Corros. **59**, 685 (2008)
7. A. Shaban, E. Kalman, I. Biczo, Corros. Sci. **35**, 1463 (1993)
8. J. Telegdi, M.M. Shaglouf, A. Shaban, F.H. Karman, I. Betroti, M. Mohai, E. Kalman, Electrochim. Acta **46**, 3791 (2001)
9. N. Ochoa, G. Baril, F. Moran, N. Pebere, J. Appl. Electrochem. **32**, 497 (2002)
10. I. Sekine, Y. Hirakawa, Corrosion **42**, 272 (1986)
11. Y.I. Kuznetsov, G.V. Zinchenko, L.P. Kazanskii, N.P. Andreeva, Y.B. Makarychev, Prot. Met **43**, 648 (2007)
12. Y.I. Kuznetsov, Russian J. Electrochem. **40**, 1287 (2004)
13. H.S. Awad, Anti-Corros. Methods Mater. **52**, 22 (2005)
14. J. Jaworska, H.V. Genderen-Takken, A. Hanstveit, E. Plassche, T. Feijtel, Chemosphere **47**, 655 (2002)
15. B.V. Appa Rao, S. Srinivasa Rao, M. Venkateswara Rao, Corros. Eng. Sci. Technol. **43**, 46 (2008)
16. B.V. Appa Rao, S. Srinivasa Rao, Mater. Corros. **61**, 285 (2010)
17. B.V. Appa Rao, M. Venkateswara Rao, S. Srinivasa Rao, B. Sreedhar, Chem. Eng. Commun. **198**, 1505 (2011)
18. B.V. Appa Rao, M. Venkateswara Rao, S. Srinivasa Rao, B. Sreedhar, J. Surf. Eng. Mater. Adv. Technol. **3**, 28 (2013)
19. M. Prabakaran, S. Ramesh, V. Periasamy, Res. Chem. Intermed. **39**, 3507 (2013)
20. K.D. Demadis, S.D. Katarachia, M. Koutmos, Inorg. Chem. Commun. **8**, 254 (2005)
21. Y. Gonzalez, M.C. Lafont, N. Pebere, F. Moran, J. Appl. Electrochem. **26**, 1259 (1996)
22. N. Nakayama, Corros. Sci. **42**, 1897 (2000)
23. J.L. Fang, Y. Li, X.R. Ye, Z.W. Wang, Q. Liu, Corrosion **49**, 266 (1993)
24. N. Labjar, M. Lebrini, F. Bentiss, N.-E. Chihib, S. El Hajjaji, C. Jama, Mater. Chem. Phys. **119**, 330 (2010)
25. P.K. Kar, Gurmeet Singh, ISRN Mater. Sci. **2011**, 1 (2011)
26. Y.V. Balaban-Irmenin, A.M. Rubashov, N.G. Fokina, Prot. Met **42**, 133 (2006)
27. S.H. Wang, C.S. Liu, F.J. Shan, G.C. Qi, Acta Metall. Sin. (Engl. Lett.) **21**, 355 (2008)
28. D. Sarada Kalyani, M. Sarath Babu, S. Srinivasa Rao, Int. J. Eng. Res. Technol. **1**, 1 (2012)
29. J.E. Singley, B.A. Beaudet, P.H. Markey, D.W. DeBerry, J.R. Kidwell, D.A. Malish, *Corrosion Prevention and Control in Water Treatment and Supply Systems* (Noyes Publications, New Jersey, 1985)
30. M. Elachouri, M.S. Hajji, M. Salem, S. Kertit, J. Aride, R. Coudert, E. Essassi, Corrosion **52**, 103 (1996)
31. S. Rajendran, B.V. Appa Rao, N. Palaniswamy, Bull. Electrochem. **17**, 171 (2001)
32. S. Rajendran, B.V. Appa Rao, N. Palaniswamy, Anti-Corros. Methods Mater. **46**, 23 (1999)
33. S.J. Yuan, S.O. Pehkonen, Corros. Sci. **49**, 1276 (2007)
34. P. Pawar, A.B. Gaikwad, P.P. Patil, Electrochim. Acta **52**, 5958 (2007)
35. C.T. Wang, S.H. Chen, H.Y. Ma, N.X. Wang, J. Serb. Chem. Soc. **67**, 685 (2002)
36. A. Bonnel, F. Dabosi, C. Deslouis, M. Duprat, M. Keddam, B. Tribollet, J. Electrochem. Soc. **130**, 753 (1983)
37. I. Felhosi, J. Telegdi, G. Palinkas, E. Kalman, Electrochim. Acta **47**, 2335 (2002)
38. J.F. Moulder, W.F. Stickle, P.E. Sobol, K.D. Bamben, *Handbook of X-Ray Photoelectron Spectroscopy: A Reference Book of Standard Spectra for Identification and Interpretation of XPS Data* (Physical Electronics, USA, 1995)
39. E. Kalman, F.H. Karman, I. Cserny, L. Kover, J. Telegdi, D. Varga, Electrochim. Acta **39**, 1179 (1994)
40. N.S. McIntyre, D.G. Zetaruk, Anal. Chem. **49**, 1521 (1977)
41. S. Maroie, M. Savy, J.J. Verbist, Inorg. Chem. **18**, 2560 (1979)
42. K. Asami, K. Hashimoto, S. Shimodaira, Corros. Sci. **16**, 35 (1976)
43. M. Koudelka, J. Sanchez, J. Augustynski, J. Electrochem. Soc. **129**, 1186 (1982)
44. M. El Azhar, M. Traisnel, B. Mernari, L. Gengembre, F. Bentiss, M. Lagrenee, Appl. Surf. Sci. **185**, 197 (2002)

45. A. Meneguzzi, C.A. Ferreira, M.C. Pham, M. Delamar, P.C. Lacaze, Electrochim. Acta **44**, 2149 (1999)
46. G.P. Cicileo, B.M. Rosales, F.E. Varela, J.R. Vilche, Corros. Sci. **41**, 1359 (1999)
47. G. Gunasekaran, L.R. Chauhan, Electrochim. Acta **49**, 4387 (2004)
48. K. Aramaki, T. Shimura, Corros. Sci. **45**, 2639 (2003)
49. F.H. Karman, I. Felhosi, E. Kalman, I. Cserny, L. Kover, Electrochim. Acta **43**, 69 (1998)
50. X.H. To, N. Pebere, N. Pelaprat, B. Boutevin, Y. Hervaud, Corros. Sci. **39**, 1925 (1997)
51. H. Amar, J. Benzakour, A. Derja, D. Villemin, B. Moreau, T. Braisaz, A. Tounsi, Corros. Sci. **50**, 124 (2008)
52. R.O. Carter, C.A. Gierczak, R.A. Dickie, Appl. Spectrosc. **40**, 649 (1986)
53. G. Gunasekaran, N. Palaniswamy, B.V. Appa Rao, V.S. Muralidharan, Electrochim. Acta **42**, 1427 (1997)
54. S. Yu, G.M. Chow, J. Mater. Chem. **14**, 2781 (2004)
55. L.J. Bellamy, *Advances in Infrared Group Frequencies* (The Chaucer Press Limited, Great Britain, 1968)
56. J.-G. Mao, A. Clearfield, Inorg. Chem. **41**, 2319 (2002)
57. Y.I. Kuznetsov, in *Proceedings of The European Corrosion Congress (EUROCORR 2003)*, Budapest, Hungary (2003), p. 320
58. A.J. Freedman, Mater. Perform. **23**, 9 (1984)
59. M. Papadaki, K.D. Demadis, Comment Inorg. Chem. **30**, 89 (2009)
60. K.D. Demadis, C. Mantzaridis, R.G. Raptis, G. Mezei, Inorg. Chem. **44**, 4469 (2005)
61. K.D. Demadis, C. Mantzaridis, P. Lydoudis, Ind. Eng. Chem. Res. **45**, 7795 (2006)
62. K.D. Demadis, P. Lykoudis, R.G. Raptis, G. Mezei, Cryst. Growth Des. **6**, 1064 (2006)
63. K.D. Demadis, M. Papadaki, R.G. Raptis, H. Zhao, Chem. Mater. **20**, 4835 (2008)
64. K.D. Demadis, E. Barouda, N. Stavgianoudaki, H. Zhao, Cryst. Growth Des. **9**, 1250 (2009)
65. K.D. Demadis, M. Papadaki, I. Cisarova, Appl. Mater. Interfaces **2**, 1814 (2010)
66. I. Felhosi, E. Kalman, P. Poczik, Russian J. Electrochem. **38**, 230 (2002)
67. V. Deluchat, J.-C. Bollinger, B. Serpaud, C. Caullet, Talanta **44**, 897 (1997)
68. K.D. Demadis, P. Lykoudis, Bioinorg. Chem. Appl. **3**, 135 (2005)